Sub Topic: IC Engines

10th U.S. National Combustion Meeting
Organized by the Eastern States Section of the Combustion Institute
April 23–26, 2017
College Park, Maryland

Working fluid replacement in gaseous direct-injection internal combustion engines: A fundamental and applied experimental investigation

Miguel Sierra-Aznar[1,], Daniel I. Pineda[1,†], Bradley S. Cage[1], Xian Shi[1], Johnathan P. Corvello[1], Jyh-Yuan Chen[1], Robert W. Dibble[1,2]*

[1]*Department of Mechanical Engineering, University of California, Berkeley, United States*
[2]*Clean Combustion Research Center, KAUST, Saudi Arabia*
[*]*Corresponding author:* m.sierra.aznar@berkeley.edu

Replacing air with argon theoretically allows for large thermal efficiency increases in internal combustion engines. Before such cycles can be realized, fundamental research on fuel injection into argon and laboratory-scale engine tests are needed. We investigated non-reacting methane jets into argon and nitrogen atmospheres in a constant volume chamber using high-speed schlieren imaging. We subsequently assessed the feasibility of methane direct-injection in a modified single cylinder research engine with an argon-oxygen mixture as the working fluid. We compared engine performance by measuring fuel flow, in-cylinder pressure, torque, and emissions. Results show that the penetration depth and spread angles of methane jets are notably different but not significantly reduced in argon compared to nitrogen. Additionally, running the modified engine with an argon-oxygen mixture in compression ignition operation leads to improvements in efficiency up to 50 percent relative to spark-ignited air cycles, and NO_X emissions are nearly eliminated. The results encourage more studies in which the exhausted argon is recycled into the intake.
Keywords: Working fluid replacement, Gaseous direct injection, Compression ignition

1 Introduction

As California installs more wind and solar power to meet its renewable energy goals by 2030, the state will need to install variable load power generation facilities to balance the load when the sun or wind varies in intensity. Gas turbines, though currently the most efficient available natural gas technology, are particularly well-suited only for a small range of loads and speeds. Alternatively, reciprocating internal combustion engines have a wider range of operation and can better meet this variable demand. According to thermodynamic theory [1], replacing the nitrogen in the working fluid of heat engines with a monatomic gas, such as argon, is a promising solution to achieve higher efficiency in power generation. Previous research by Killingsworth et al. [2] focused on H_2-O_2-Ar combustion, and demonstrated large (30–35%) relative efficiency gains for a given compression ratio, r_c. However, engine knock limited increases in compression ratio and thus limited efficiency gains. Modern gaseous direct-injection strategies with more knock-resistant fuels such as CH_4

[*]Corresponding author, m.sierra.aznar@berkeley.edu
[†]Presenting author, dpineda@berkeley.edu

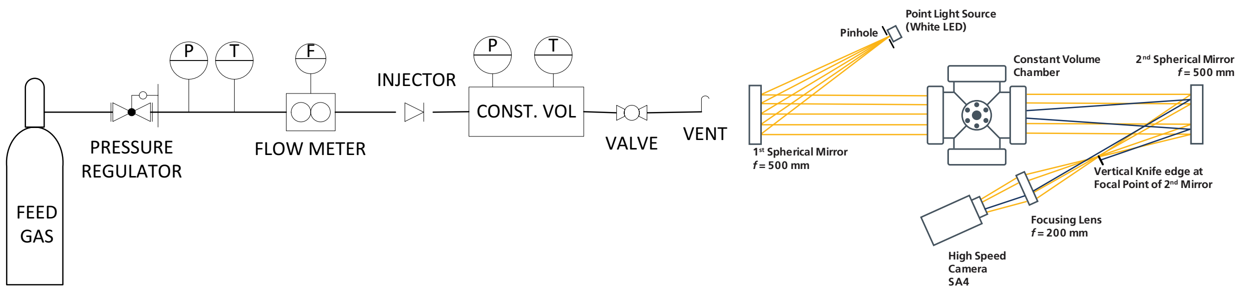

Figure 1: Small constant volume chamber for mass flow measurements (left) and top-view of the schlieren setup with the larger optically accessible constant volume chamber in the laboratory (right).

can overcome these obstacles to achieve greater engine efficiency, but fundamental and applied research is needed to demonstrate the feasibility of such an approach using both port fuel injection (PFI) spark ignition (SI) and compression ignition (CI) through direct injection (DI). In this investigation, we document the use of CH_4 DI strategies in Ar-based atmospheres with data from both constant-volume chamber experiments and single-cylinder engine experiments.

2 Method

We constructed two separate constant volume chamber experiments to characterize injection behavior. To determine the mass of fuel injected per injection, we assembled a small constant volume chamber attached to the injector with a pressure sensor, as shown in the left of Figure 1. By measuring the pressure in the chamber as a function of time, we determined the mass of fuel injected across a continuous range of pressure differences between injection and chamber pressure. Moreover, steady state mass flow rate of the injector was also measured at a constant pressure drop from injection pressure to atmospheric pressure. We conducted these tests with three different inert gases (Ar, N_2, and He) to avoid fire hazards when purging the gases out of the chamber; these specific gases were chosen to cover a wide range of molecular weights. We then used the results to estimate the mass injection rate of CH_4. A comparison to theoretical values obtained using the ideal gas law could be drawn. The average discharge coefficients were deduced from the data to approximate the real mass flow of the fluids of interest through the injector under choked flow.

To characterize the opening and closing error in the injector and to estimate the jet penetration and spread angle experimentally, we tested the injector in a larger constant volume chamber (1.45 L) with optical access for high-speed schlieren imaging, illustrated on the right in Figure 1. More detailed information on the camera and chamber setup can be found in previous research [3, 4]. Images were recorded at $f = 3600$ Hz with a shutter speed of 25 μs. The high-speed imaging enabled determination of how accurately the injector followed given commands. Non-reacting experiments were conducted injecting CH_4 at 100 ± 0.05 bar into a chamber filled with either Ar or N_2 at 10 ± 0.05 bar with an injection duration of 5 ms. The chamber pressure was chosen to match the number density expected at engine conditions (40 bar, 1200 K). The spread angles and penetration depths were analyzed using an in-house MATLAB image-processing code.

For the engine experiments, we used a modified single cylinder variable compression ratio Cooperative Fuel Research (CFR) engine (Waukasha Motor Company [5]). Details about the engine specifications can be found in the work by Rapp et al. [6], and a more complete account of our modifications can be found in our report to the California Energy Commission [7]. For all tests, the engine speed was kept constant at 600 rpm and the intake manifold was kept at 1 bar absolute pressure. The techniques to determine Indicated Mean Effective Pressure (IMEP), Coefficient of Variation of IMEP (COV_{IMEP}), indicated specific fuel consumption (ISFC), and indicated thermal efficiency η_{th} from the data follow the methods of Rapp et al. [6] and will not be discussed here.

For PFI-SI operation, we conducted a series of engine simulations (in-house 2-zone model based on code used by Killingsworth et al. [2]) to establish feasible bounds on r_c and Ar dilution for SI operation. We found that maximum η_{th} could be expected at r_c = 6–10 with an oxidizer comprising 85% Ar-15% O_2. We ran the CFR engine with CH_4 and air at $\phi = 1$ and r_c = 6–12 to establish a baseline. Then we ran with CH_4 and Ar-O_2 mixtures holding r_c constant at 6 and varying O_2 content to explore the performance enhancement. After experimentally confirming the optimum O_2 content, we ran CH_4 and Ar-O_2 mixtures for r_c up to 10. All reported PFI-SI engine results represent Maximum Brake Torque (MBT) θ_{ign}, that is, the θ_{ign} that results in the greatest amount of torque output to the dynamometer [8].

For DI-CI operation, we increased the r_c of the engine. CH_4 is difficult to auto-ignite, but the high temperatures resulting from compressing Ar make CI operation with CH_4 possible. Similar to the PFI-SI operation, we performed DI-CI engine simulations using a commercial code (CONVERGE [9]) to narrow the feasible experimental operating range. We estimated the minimum temperature needed for auto-ignition to be 1200 K, which is achievable with $r_c \geq 14$ and an injection timing of θ_{inj} = 30–25°CA bTDC with about 30 mg of CH_4 injected per cycle. Once the DI experimental parameters had been narrowed, we proceeded to use the injector in the engine with CH_4 and an oxidizer of 15% O_2-85% Ar. Due to the low reactivity of CH_4, reliable combustion under DI-CI operation was not obtained until $r_c \geq 15$. However, we were able to use spark-assisted compression ignition (SACI) to achieve stable DI operation at $r_c = 14$.

3 Results

The constant volume chamber results helped to inform the engine operation. Based on the outcomes of injection mass flow experiments for N_2, Ar, and He, we calculated the resulting discharge coefficient of the injector to be $C_D = 0.11$. The transient pressure measurement results indicate that that for CH_4 at 100 bar, the flow through the injector is 624 mg/s. For the CFR engine running at 600 rpm, the injection duration for 30 mg of CH_4 would be 88 °CA for stoichiometric mixtures with an oxidizer comprising 20% O_2. Though this duration is feasible for ignition, we confirmed that the engine performance would be limited by the burning rate as a consequence.

For the schlieren imaging results, our specified injection duration (5 ms) resulted in approximately 3 mg of CH_4 injected per experiment. The imaging results reveal that, relative to N_2 atmospheres, the penetration depth of CH_4 jets are notably but not significantly reduced in an Ar atmosphere, as shown in Figure 2. Nominally, a slightly wider spread angle (26.06 ± 4.04°) is observed for CH_4 injection in Ar than in N_2 (24.58 ± 2.88°), but the uncertainties indicate there is no substantial difference between the injection of CH_4 in Ar and N_2. Entrainment in Ar atmospheres is larger than in N_2 atmospheres due to Ar's higher molecular weight, enhancing fuel-oxidizer mixing.

For the engine results, a summary of the PFI-SI operation outcomes for $r_c = 6$ at θ_{ign} = MBT is

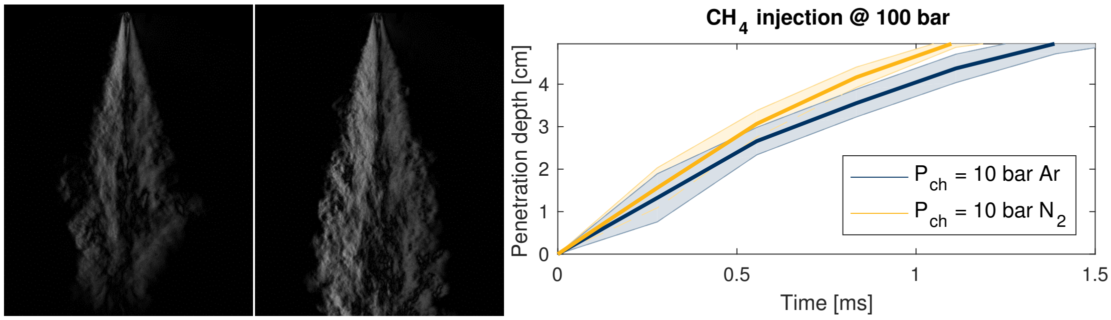

Figure 2: Representative high-speed images of CH_4 jets injected from 100 bar into Ar and N_2 at 10 bar (left) and calculated penetration depths (right). Shaded regions indicate 90% confidence intervals.

Table 1: Summary of PFI-SI CFR engine results. $r_c = 6$ and $\phi = 1$ for all conditions.

O_2 content [%]	IMEP [bar]	COV_{IMEP} [%]	ISFC [g/kWh]	η_{th} [%]	THC [ppm]	NO_X [ppm]
21 (79% N_2)	6.92	2.5	261.4	27.5	1442	1510
10 (90% Ar)	5.49	8.0	191.2	37.7	1821	2.1
15 (85% Ar)	7.33	3.3	199.6	36.1	1425	4.5
20 (80% Ar)	8.42	1.9	209.2	34.6	1071	13.8

presented in Table 1 with key engine performance parameters listed. The levels of COV_{IMEP} are all acceptably below 5%, except for the 10% O_2 case with $COV_{IMEP} = 8\%$. The poor engine stability for the 10% O_2 case is consistent with our modeling assessment, in which we faulted low flame speeds. In the left of Figure 3, example plots are presented for measured in-cylinder pressure traces as a function of θ for the four PFI-SI cases in Table 1. We then evaluated the influence of r_c on the overall η_{th} of the cycle. In the center of Figure 3, it can be seen that—for a given r_c—the engine achieves higher η_{th} with Ar than air as the working fluid.

Table 2 summarizes the results of four DI experiments using $r_c \geq 14$, and representative pressure traces are shown in the right of Figure 3. Although the mean peak pressure nears 80 bar at $r_c = 14$, the ISFC, as shown in Table 2, only decreased to 195.2 g/kWh for $\phi = 1$. The emission data in Table 2 show no evidence of increase in THC (remaining < 800 ppm), suggesting that combustion is not incomplete. Less than 10 ppm of NO_X is observed, indicating that the system has no air leaking into the engine. The best engine performance is observed with DI-SACI operation for $\phi = 0.74$ and $\theta_{ign} = 10$ °CA BTDC with a 50% improvement in indicated thermal efficiency relative to the air-breathing PFI-SI case at $r_c = 12$. An examination of the heat release rate (HRR) reveals that the relatively limited improvement during DI operation for $\phi = 1$ was caused by inadequate combustion phasing. For $\phi = 1$, the required amount of CH_4 corresponds to an injection

Table 2: Summary of DI CFR engine results. $\theta_{inj} = 30$°CA bTDC and oxidizer 15% O_2-85% Ar for all conditions.

r_c	ϕ	θ_{ign} [°CA]	IMEP [bar]	COV_{IMEP} [%]	ISFC [g/kWh]	η_{th} [%]	THC [ppm]	NO_X [ppm]
15	1.00	N/A	6.11	4.5	211.8	34.0	597	7.6
14	1.00	N/A	6.35	3.9	203.8	35.3	729	6.4
14	1.00	-10	6.33	3.3	195.2	36.9	465	8.6
14	0.74	-10	7.29	4.0	162.9	44.2	219	18.3

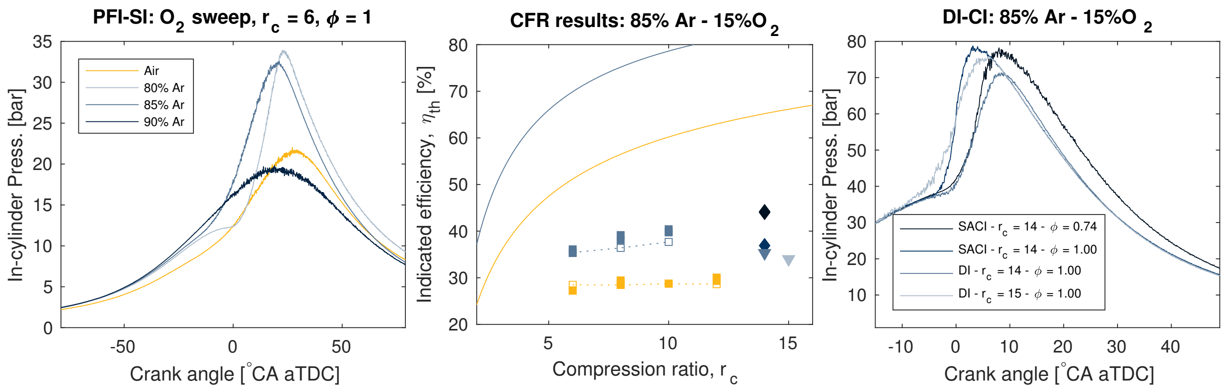

Figure 3: Pressure traces for the O_2 sweep for PFI-SI operation at $r_c = 6$ (left), η_{th} as a function of r_c for all PFI-SI, DI, and SACI 85% Ar-15% O_2 runs (center), and pressure traces for DI tests (right). Air runs in gold, Ar runs in blue. In the center plot, squares are PFI-SI runs, triangles are DI runs, and diamonds are SACI runs. Solid markers are experiments, open markers are 2-zone simulations, and solid lines correspond to ideal Otto cycle calculations.

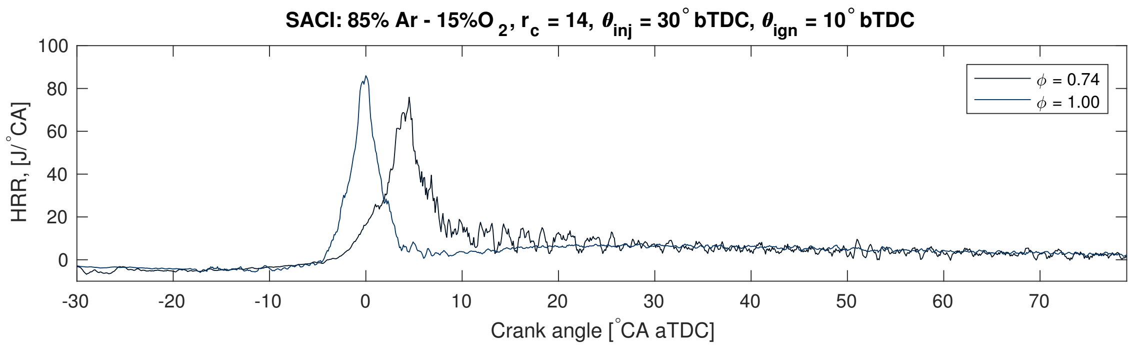

Figure 4: Representative samples of heat release rate for SACI operation with varying ϕ.

duration of approximately 60 °CA. The HRR of a representative stoichiometric DI-SACI cycle is presented in Figure 4. A sudden heat release occurs after ignition near TDC, but quickly transitions to a slow heat release event. This is caused by injector limitations that constrain the maximum fuel flow rate. We explored DI-SACI operation at leaner conditions ($\phi = 0.74$) to achieve better combustion phasing, as shown in the right of Figure 3 and Figure 4, resulting in $\eta_{th} = 44.2\%$.

4 Conclusion

In this study, we evaluated the potential improvement in thermal efficiency of an internal combustion engine through the replacement of nitrogen with argon as the working fluid. We characterized an experimental gaseous direct injector and did not find major differences between methane injection events in argon and nitrogen atmospheres. Slightly lower penetration was observed in argon, but the difference was not substantial. Similarly, results regarding spread angles did not reveal any major difference, and thus we assume research and development on gaseous direct injection in air atmospheres can apply to argon atmospheres. We were able to achieve stable engine operation under both spark ignition and compression ignition operation modes. 15% O_2-85% Ar was found as the optimal oxidizer mixture, achieving an efficiency gain of 34% relative to the air-breathing case at the same compression ratio. Results from the direct injection engine experiments showed that the operational range of the engine could be expanded, and stable operation of the engine was achieved at compression ratios up to 14. Indicated thermal efficiencies of up to 44% were achieved, corresponding to a 50% improvement in efficiency relative to the air-breathing port fuel injected spark ignition case at a compression ratio of 12. In regards to the unburned hydrocarbons, all argon cycles produced less than 800 ppm, corresponding to a 50% reduction relative to air operation ($\sim$1400 ppm). For NO_X, the argon cycles demonstrated a 99% reduction relative to spark ignition air operation. Our results encourage future research in which the cycle is in a closed loop, recycling the exhausted argon into the intake and separating CO_2 via membranes between cycles. Additionally, we expect more reliable operation as gaseous direct injection technology matures.

Acknowledgments

The research was funded in part by the California Energy Commission: Energy Innovations Small Grant No. 5804A/14-07G, and by the King Abdullah University of Science and Technology, Subaward Agreement Ref. No. OSR-2016-CPF-2909-02. The construction of the experiment was made possible by the donation of fuel injection and piping equipment by Bosch and Parker Hannifin, respectively. The authors thank Charles Scudiere for setting up and running the CONVERGE simulations. The authors would like to acknowledge Michael Neufer and Alex Jordan of the Technical and Instructional Support Group of the Department of Mechanical Engineering for their expertise in assembling and operating the Cooperative Fuel Research engine. MSA also wishes to thank Malte Schäfer for his assistance in the construction of the engine, Tim Sennott for his help during the injection experiments and Florian Courbin for his help manufacturing the injector adapters. DIP thanks Jordan Yvette Nerison for the final illustration in Figure 1.

References

[1] Michael J. Moran and Howard N. Shapiro. *Fundamentals of Engineering Thermodyamics*. John Wiley & Sons, Inc., New York, NY, 4th edition, 2000.

[2] Nick J. Killingsworth, Vi H. Rapp, Daniel L. Flowers, Salvador M. Aceves, J. Y. Chen, and Robert Dibble. *Proc. Combust. Inst.*, 33 (2011) 3141–3149.

[3] Daniel I. Pineda, Benjamin Wolk, Tim Sennott, Jyh-Yuan Chen, Robert W. Dibble, and Daniel R. Singleton. Nanosecond Pulsed Discharge in a Lean Methane-Air Mixture. In *Laser Ignition Conf.*, Vol. C, page T5A.2, Lemont, IL, 2015. Argonne National Laboratory, OSA Publishing.

[4] Benjamin Wolk, Anthony C. DeFilippo, Jyh-Yuan Chen, Robert W. Dibble, Atsushi Nishiyama, and Yuji Ikeda. *Combust. Flame*, 160 (2013) 1225–1234.

[5] ASTM International. ASTM D2699-16, Standard Test Method for Research Octane Number of Spark-Ignition Engine Fuel, 2016.

[6] Vi H. Rapp, Anthony C. DeFilippo, Samveg Saxena, Jyh-Yuan Chen, Robert W. Dibble, Atsushi Nishiyama, Ahsa Moon, and Yuji Ikeda. *J. Combust.*, 2012 (2012) 1–8.

[7] J.-Y. Chen, Daniel I. Pineda, M. Sierra-Aznar, and X. Shi. Maximizing Efficiency of Natural Gas Engines Through Argon Power Cycle. Technical Report EISG Grant No. 58074A/14-07G, California Energy Commission, Sacramento, CA, 2017.

[8] John B. Heywood. *Internal Combustion Engine Fundamentals*. McGraw-Hill, 1st edition, 1988.

[9] K. J. Richards, P. K. Senecal, and E. Pomraning. CONVERGE, 2016.